

Stereoscopic Correspondence by Applying Physical Constraints and Statistical Observations to Dissimilarity Map

T.-Y. Chao^a, S.-J. Wang^b and H.-M. Hang^c

^{abc} Dept. of Electronics Engineering,
National Chiao Tung University,
Hsinchu, Taiwan 30010, ROC

ABSTRACT

To deal with the correspondence problem in stereo imaging, a new approach is presented to find the disparity information on a newly defined dissimilarity map (DSMP). Based on an image formation model of stereo images and some statistical observations, two constraints and four assumptions are adopted. In addition, a few heuristic criteria are developed to define a unique solution. All these constraints, assumptions and criteria are applied to the DSMP to find the correspondence. At first, the Epipolar Constraint, the Valid Pairing Constraint and the Lambertian Surface Assumption are applied to DSMP to locate the Low Dissimilarity Zones (LDZs). Then, the Opaque Assumption and the Minimum Occlusion Assumption are applied to LDZs to obtain the admissible LDZ sets. Finally, the Depth Smoothness Assumption and some other criteria are applied to the admissible LDZ sets to produce the final answer. The focus of this paper is to find the constraints and assumptions in the stereo correspondence problem and then properly convert these constraints and assumptions into executable procedures on the DSMP. In addition to its ability in estimating occlusion accurately, this approach works well even when the commonly used monotonic ordering assumption is violated. The simulation results show that occlusions can be properly handled and the disparity map can be calculated with a fairly high degree of accuracy.

Keywords: Epipolar Constraint, Valid Pairing constraint, Lambertian Surface Model, Opaque Assumption, low dissimilarity zone, disparity, depth.

1. INTRODUCTION

Finding pixel correspondence in stereo image pairs is an important but difficult issue in geometric stereo. Many papers¹⁻⁵ have discussed the correspondence issue and their methods can be roughly classified into two classes: feature-based methods and intensity-based methods. Feature-based methods use the object features in an image pair to generate a quite reliable but sparse disparity map. Intensity-based methods use the image intensity information to produce a denser disparity map. Since feature-based methods only use partial information of the image pair, we adopt an intensity-based approach in this paper to fully utilize all the information of the image pair. Our method is developed based on the notion of dissimilarity map (DSMP). DSMP is a new concept; it measures the dissimilarity between a pair of stereo images. As shown in Figure 1, Our DSMP-based method includes the geometric constraints, the photometric assumptions, and the statistical assumptions on DSMP to find the pixel correspondence. These geometric constraints are consist of the Epipolar Constraint and the Valid Pairing Constraint; the photometric assumptions are consist of the Lambertian Surface Model Assumption and the Opaque Assumption; and the statistical assumptions are consist of the Minimum Occlusion Assumption and the Depth Smoothness Assumption. In this paper, the preceding constraints and assumptions are converted into practical procedures operated on DSMP. The basic theory is first developed assuming the image has infinite resolution and the noise is absent. Then the noise interference and the projective distortion due to the finite resolution of a real image is investigated and some modifications on the correspondence operations are made.

Further author information:

Tsi Yi Chao: E-mail: u8411824@cc.nctu.edu.tw

S.-J. Wang: E-mail: shengjyh@cc.nctu.edu.tw

H.-M. Hang: E-mail: hmhang@cc.nctu.edu.tw

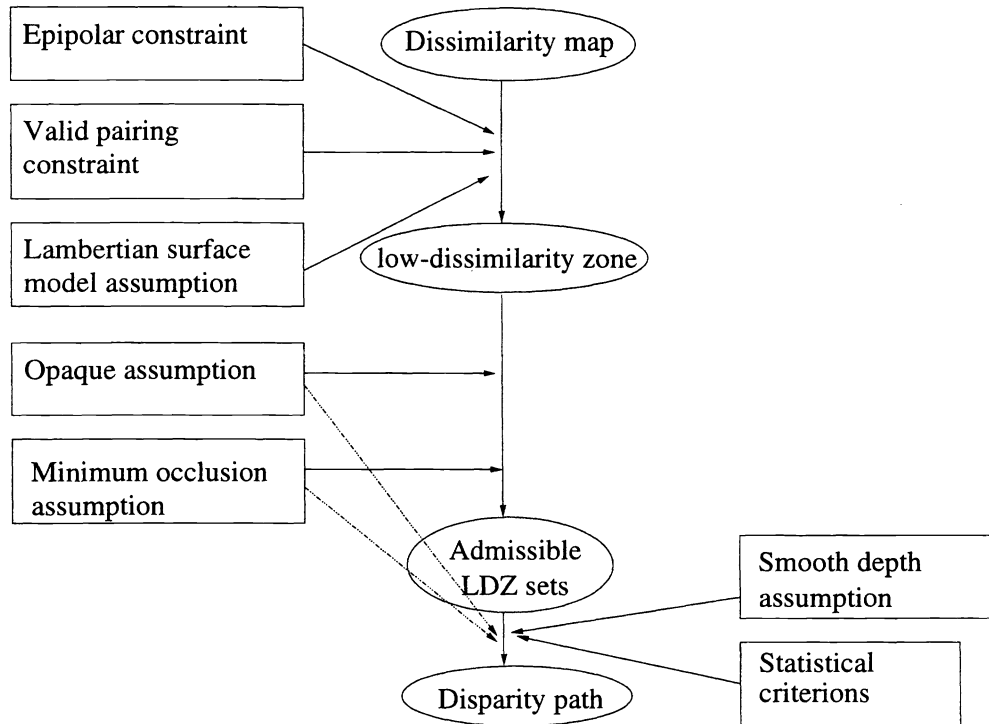


Figure 1. The flow diagram of DSMP method

2. GEOMETRIC MODEL

2.1. Projection Model

The projection mechanism of a camera can be modeled as a perspective projection as shown in Figure 2. In this figure, there are two coordinate systems, (X_i, Y_i) and (x, y, z) . (X_i, Y_i) represents the coordinates of a projected point on the image plane. By using triangular similarity, we have

$$\frac{X_i}{f} = -\frac{x}{z} \quad \text{and} \quad \frac{Y_i}{f} = -\frac{y}{z}.$$

If we define the new coordinates to be: $X_m = -X_i$ and $Y_m = -Y_i$, then

$$\frac{X_m}{f} = \frac{x}{z} \quad \text{and} \quad \frac{Y_m}{f} = \frac{y}{z}. \quad (1)$$

The above transformation simply translates the original image to its mirror image with respect to the lens center (from (X_i, Y_i) to (X_m, Y_m) as shown in Figure 2). That is, we deal with the mirror image, instead of the image plane, to simplify the transformation expression.

2.2. Stereoscopic Camera System Model

A stereoscopic camera system¹ is shown in Figure 3. The line B connecting two projection centers of projection is called the **baseline**. In addition, f represents the focal length and θ represents the convergence angle ($0^\circ \leq \theta < 180^\circ$). In Figure 3, we have three coordinates: left, center, and right. Equations (2) is derived to relate the left coordinates with right coordinates.¹

$$\begin{bmatrix} x_r \\ y_r \\ z_r \end{bmatrix} = \begin{bmatrix} \cos \theta & 0 & \sin \theta \\ 0 & 1 & 0 \\ -\sin \theta & 0 & \cos \theta \end{bmatrix} \times \begin{bmatrix} x_l \\ y_l \\ z_l \end{bmatrix} + \begin{bmatrix} -B \cos \frac{\theta}{2} \\ 0 \\ B \sin \frac{\theta}{2} \end{bmatrix}. \quad (2)$$

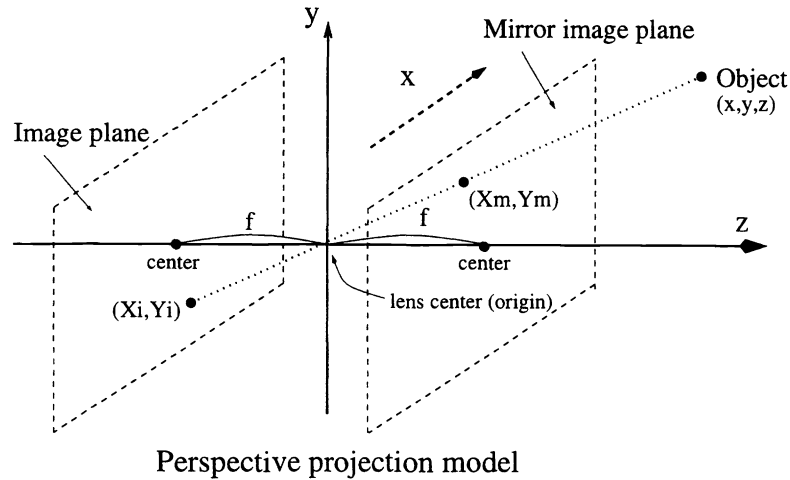


Figure 2. Perspective Projection model and It's Coordinate Translation

Combining (1) and (2), we can derive

$$z_l = \frac{B(f \cos \frac{\theta}{2} + X_{m_r} \sin \frac{\theta}{2})}{f \sin \theta + \frac{\sin \theta}{f} X_{m_l} X_{m_r} + \cos \theta (X_{m_l} - X_{m_r})}. \quad (3)$$

$$z_r = \frac{B(f \cos \frac{\theta}{2} - X_{m_l} \sin \frac{\theta}{2})}{f \sin \theta + \frac{\sin \theta}{f} X_{m_l} X_{m_r} + \cos \theta (X_{m_l} - X_{m_r})}. \quad (4)$$

Therefore, if the (X_{m_l}, X_{m_r}) pair in the conjugate epipolar lines is known, z_l and z_r (depth) can be found by using (3) and (4). To find the depth information, we match (X_{m_l}, X_{m_r}) first and then substitute (X_{m_l}, X_{m_r}) into Equations (3) to calculate the depth information. The variable z_l is used to denote the depth. Furthermore, the disparity is defined as $D_m = (X_{m_l} - X_{m_r})$. When $\theta = 0$, Equation (3) degenerates to

$$z_l = \frac{Bf}{X_{m_l} - X_{m_r}} = \frac{Bf}{D_m}. \quad (5)$$

3. GEOMETRIC CONSTRAINTS

The geometric constraints include the Epipolar Constraint and the Valid Pairing Constraint. The geometric constraints are derived based on the calibration of the left and the right cameras. Any matching point must obey the geometric constraint.

3.1. Epipolar line constraint

Consider a pair of images. Let Pl and Pr denote the projections of a real world 3-D point p onto the left and right image planes, respectively. Let Ol and Or denote the corresponding centers of the pinhole projection model. A plane that passes through these two centers of projection is called an **epipolar plane**. Each epipolar plane intersects with both mirror image planes and these intersections are called conjugate (or corresponding) **epipolar lines**⁶ (Figure 4).

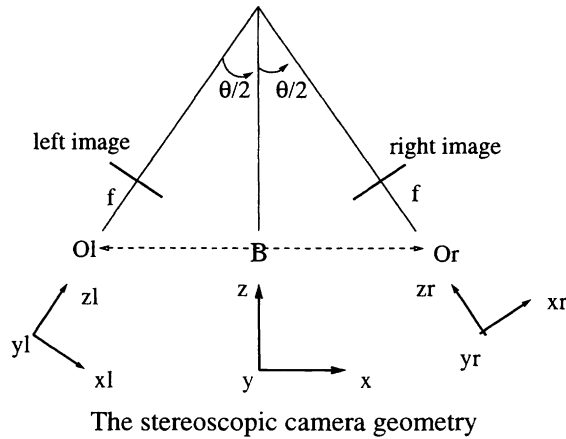


Figure 3. The stereoscopic camera geometry

3.2. Valid pairing constraints

Valid Pairing Constraint describes the constraint on Xm_l and Dm under the condition that the object at Xm_l and Dm can be seen by both the left and right cameras with a complete viewing angle.

Substitute $Dm = (Xm_l - Xm_r)$ into Equations (3) and (4), we get

$$z_l = \frac{B(f \cos \frac{\theta}{2} + (Xm_l - Dm) \sin \frac{\theta}{2})}{f \sin \theta + \frac{\sin \theta}{f} Xm_l (Xm_l - Dm) + Dm \cos \theta}, \quad (6)$$

$$z_r = \frac{B(f \cos \frac{\theta}{2} - Xm_l \sin \frac{\theta}{2})}{f \sin \theta + \frac{\sin \theta}{f} Xm_l (Xm_l - Dm) + Dm \cos \theta}, \quad (7)$$

where z_l and z_r must be positive due to the camera's structure. Hence, we can derive the restriction on Dm as

$$\begin{cases} (Xm_l - Dm) > -f \cot \frac{\theta}{2} \text{ and } Xm_l < f \cot \frac{\theta}{2} & \Rightarrow (f \sin \theta + \frac{\sin \theta}{f} Xm_l (Xm_l - Dm) + Dm \cos \theta) > 0 \\ (Xm_l - Dm) < -f \cot \frac{\theta}{2} \text{ and } Xm_l > f \cot \frac{\theta}{2} & \Rightarrow (f \sin \theta + \frac{\sin \theta}{f} Xm_l (Xm_l - Dm) + Dm \cos \theta) < 0. \end{cases}$$

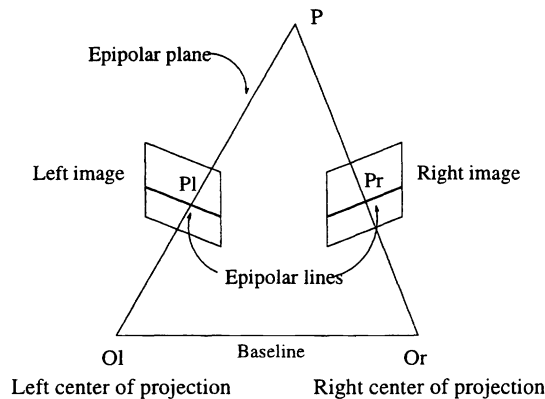


Figure 4. Epipolar plane and epipolar lines

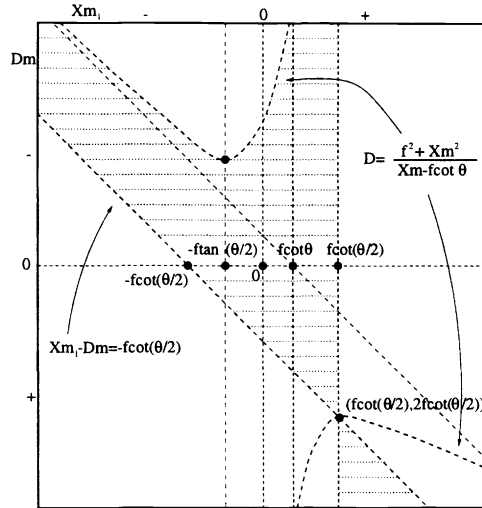


Figure 5. Valid pairing constraint

Reorganize the above constraints on Dm , we get

$$\left\{ \begin{array}{ll} (Xm_l - Dm) > -f \cot \frac{\theta}{2} \text{ and } Xm_l < f \cot \theta, & \Rightarrow Dm > \frac{Xm_l^2 + f^2}{Xm_l - f \cot \theta} \\ (Xm_l - Dm) > -f \cot \frac{\theta}{2} \text{ and } f \cot \theta < Xm_l < f \cot \frac{\theta}{2}, & \Rightarrow Dm < \frac{Xm_l^2 + f^2}{Xm_l - f \cot \theta} \\ (Xm_l - Dm) < -f \cot \frac{\theta}{2} \text{ and } Xm_l > f \cot \frac{\theta}{2}, & \Rightarrow Dm > \frac{Xm_l^2 + f^2}{Xm_l - f \cot \theta}, \end{array} \right. \quad (8)$$

where $0^\circ < \theta < 180^\circ$ and these equations are drawn in Figure 5. When $\theta = 0^\circ$, the Valid Pairing Constraint will degenerate to $Dm > 0$. Note that instead of (Xm_l, Xm_r) , we can use the equivalent pair (Dm, Xm_l) as the key parameters in the preceding equations.

4. PHOTOMETRIC ASSUMPTIONS

The photometric assumptions include the Lambertian Surface Assumption and the Opaque Assumption. The Lambertian Surface Assumption is based on the simple light model of lambertian surface. The Opaque Assumption is a very popular assumption and it is valid in most cases.

4.1. Lambertian surface model assumption

The light model is very complex in nature and is difficult to model. Here, we use a simple light model called lambertian surface model, which has the property that its radiance depends only on the incident illumination but not the viewing direction. Based on the Lambertian surface model assumption, the reflected illumination on a stereo pair from the same incident point should be the same if noises are absent.

4.2. Opaque Assumption

4.2.1. Slope constraints under monotonic ordering

Regions *I*, *II*, *III*, and *IV* are defined to be the regions separated by lines L_l and L_r as shown in Figure 6. Point *A* is the crossing point of L_l and L_r . The line L_l passing through both point *A* and the left optical center, while the line L_r passing through point *A* and the right optical center. Point *B1* or *B2* represents a neighborly unoccluded point which follows the monotonic ordering assumption with respect to *A*. The Opaque Constraint implies that points *B1* and *B2* cannot locate on lines L_l and L_r . If point *B1* is on the right side of L_l (that is the next matching point), then this point should be on the right side of L_r under the monotonic ordering assumption. Hence, the possible region for *B1* should be in Region *IV*. Similarly, if point *B2* is in the left side of L_l (that is, the previous matching

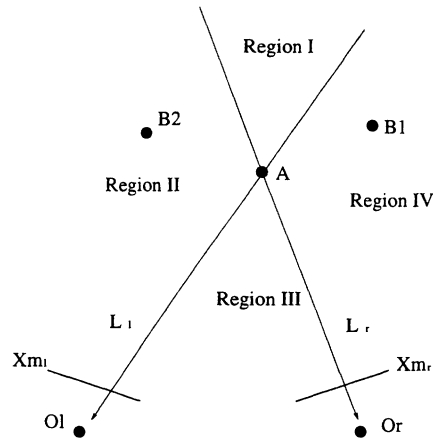


Figure 6. The slope analysis on the 3-D point under monotonic order

point), then this point should be on the left side of L_r under the monotonic ordering assumption (Region II). Thus, the only possible region of $B1$ or $B2$ should be on the same side of lines L_l and L_r (Region II and IV).

Region II and IV can be represented by

$$\begin{cases} \text{region II} : X_{m_{B1}} < X_{m_{A_l}} \text{ and } X_{m_{B_r}} < X_{m_{A_r}} \\ \text{region IV} : X_{m_{B1}} > X_{m_{A_l}} \text{ and } X_{m_{B_r}} > X_{m_{A_r}}. \end{cases} \quad (9)$$

The corresponding region of Region II and IV in the (X_{m_l}, D_m) domain can be represented by

$$\begin{aligned} & \begin{cases} D_{m_B} = X_{m_{B1}} - X_{m_{B_r}} \\ D_{m_A} = X_{m_{A_l}} - X_{m_{A_r}} \end{cases} \\ \Rightarrow \frac{D_{m_B} - D_{m_A}}{X_{m_{B1}} - X_{m_{A_l}}} &= \frac{(X_{m_{B1}} - X_{m_{A_l}}) - (X_{m_{B_r}} - X_{m_{A_r}})}{X_{m_{B1}} - X_{m_{A_l}}} \\ &= 1 - \frac{X_{m_{B_r}} - X_{m_{A_r}}}{X_{m_{B1}} - X_{m_{A_l}}} < 1. \end{aligned} \quad (10)$$

The unmatched parts under the monotonic ordering assumption are not “true occlusion” and therefore are called “pseudo occlusion” here.

4.2.2. Multi-layer description for the disparity paths in the (X_{m_l}, D_{m_l}) domain

Here, the Opaque Assumption is converted into an multi-layer description for the disparity paths in (X_{m_l}, D_m) domain and this description, which is a result of the Opaque Assumption, will be used on dissimilarity map described later to find solutions.

Assume a stereo imaging system is set up. Given a set of unoccluded 3-D points, the corresponding 2-D points in the (X_{m_l}, D_m) domain are called “disparity points”. To have an efficient description of the disparity information of these unoccluded disparity points, we developed a multi-layer description. At first, several sets of disparity points that follow the monotonic ordering assumption are extracted. Then, these sets are organized by a multi-layer structure.

In Section 4.2.1, we conclude that the unoccluded 3-D points under the monotonic ordering assumption fall in Regions II and IV. That is, the slope of the line from the current unoccluded disparity point to any neighboring unoccluded disparity point is smaller than 1. Starting from left, we pick up the leftmost disparity point in the dissimilarity map and name it $P1$. Then we search for the point $P2$, which is the leftmost point among all the disparity points that can obey the monotonic ordering assumption with respect to $P1$. We repeat the same procedure to group more and more disparity points into the set such that any added disparity point follows the monotonic ordering assumption with respect to all the disparity points included in the set. After finishing the whole procedure, we call this set “layer 1 disparity path”.

Under the Opaque Assumption, the remaining unoccluded 3-D points must violate the monotonic order with respect to the *layer 1* disparity path. Again, from the leftmost disparity point in the remaining points, we can construct “layer 2 disparity path” and so on.

5. OCCLUSION ANALYSIS AND STATISTICAL ASSUMPTIONS

The matching points must follow all the geometric constraints and photometric assumptions. Hence, all the possible matching paths follow the geometric constraints and photometric assumptions. The Epipolar Constraint is used when the conjugate epipolar lines are used in correspondence. The Valid Pairing Constraint is used to make sure that the object at (Xm_l, Dm) can be seen by both the left and right cameras. The Lambertian Surface Assumption is used to suggest that the the corresponding intensity may come from the same 3-D point. The Opaque Constraint ensures that the uniqueness of the matching points along the line of sight. From the above discussions, we know that for given conjugate epipolar lines, all the matching points in agreement with the geometric constraints and photometric assumptions are candidates on the true disparity path. Thus, we can use these constraints and assumptions to exclude the incorrect points. Then, the statistical assumptions can be used to choose the solution which has the highest probability in the real world. These constraints and assumptions come from the fundamental theory of image formation and they are crucial in helping finding the correct solution.

5.1. Occlusion analysis

Again, Region *I*, *II*, *III*, and *IV* as defined in Figure 7. Point *A* is the crossing point of L_l and L_r . Point B_i represents the possible neighboring matching point. Point B_i may fall in Regions *I*, *II*, *III* or *IV*. The location of point B_i can be classified into four categories.

- **Points A and B_i are continuous**
This case means that both the Xm_l and Xm_r coordinates of A and B_i are continuous; there is no occlusion. Point B_1 in Figure 7 belongs to this case.
- **Points A and B_i are discontinuous, but the distance of B_i to L_l is infinitely small**
This case means that only the Xm_r coordinate of A and B_i is discontinuous; there is a “right occlusion”. Point B_2 in Figure 7 belongs to this case.
- **Point A and B_i are discontinuous, but the distance of B_i to L_r is infinitely small**
This case means that only the Xm_l coordinate of A and B_i is discontinuous, there is a “left occlusion”. Point B_3 in Figure 7 belongs to this case.
- **Points A and B_i are discontinuous**
This case means that both the Xm_l and Xm_r coordinates of A and B_i are discontinuous. Both a left occlusion and a right occlusion occurs at the same time. We call this “cross-over occlusion”. Point B_4 in Figure 7 belongs to this case.

5.2. Statistical assumptions

The Statistical Assumptions include the Depth Smoothness Assumption and the Minimum Occlusion Assumption. The Depth Smoothness Assumption assumes that the depth of the scene which has a smooth intensity variation should be smooth. The Minimum Occlusion Assumption assumes that a real matching path should have minimum amount of occlusion under the geometric constraints and the photometric assumptions. This Minimum Occlusion Assumption implies that there is no cross-over occlusion whenever there is a match.

6. DISSIMILARITY MAP AND ITS APPLICATIONS

6.1. Dissimilarity map (DSMP)

We denote the intensity value in the left scanline as $I_L(Xm_l)$ and the right scanline as $I_R(Xm_r)$. Then, the dissimilarity map (DSMP) is defined to be

$$DSMP(Xm_l, D) = F(I_L(Xm_l), I_R(Xm_l - D)), \quad (11)$$

where Xm_l is the coordinate in the left scanline and D is the position shift between the left and right scanline coordinates. When noise is absent, the $F(\cdot)$ should be zero, at $D = D_c$.

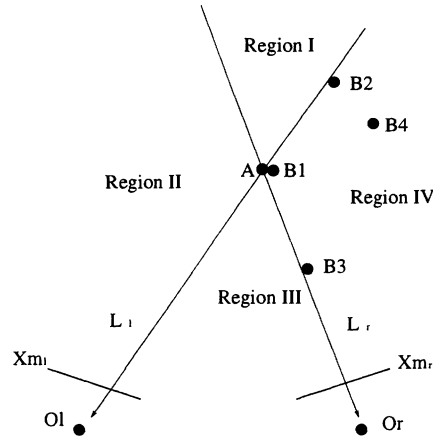


Figure 7. The occlusion analysis on the 3-D point

6.2. Lambertian surface model assumption on dissimilarity map

Suppose the corresponding matching point of Xm_l in the right scanline is Xm_r . Based on the Lambertian Surface Assumption, we have

$$F(I_L(Xm_l), I_R(Xm_l - D)) \approx 0, \quad (12)$$

Now, we define the disparity as $Xm_l - Xm_r$. When $D = D_c = Xm_l - Xm_r = \text{disparity}$,

$$DSMP(Xm_l, D_c) = F(I_L(Xm_l), I_R(Xm_l - D_c)) = F(I_L(Xm_l), I_R(Xm_r)) \approx 0 \quad (13)$$

The (Xm_l, Dm) points satisfying eqn. (13) are called the low dissimilarity zone (LDZ) in a DSMP. Ideally, the LDZ has zero $F(\cdot)$ value.

6.2.1. The shape of LDZ in DSMP

The knowledge of the shape of LDZ is useful in deciding the disparity path. Here we discuss the shape of the LDZs under the condition that $F(\cdot) = 0$ for the matching pairs.

Suppose $I_L(Xm_l) = C$ for $a_l < Xm_l < b_l$ with $I_L(a_l) \neq C$ and $I_L(b_l) \neq C$, and $I_R(Xm_r) = C$ for $a_r < Xm_r < b_r$ with $I_R(a_r) \neq C$ and $I_R(b_r) \neq C$. Then

$$DSMP(Xm_l, D) = F(I_L(Xm_l), I_R(Xm_l - D)) = 0 \quad (14)$$

when $a_l < Xm_l < b_l$ and $a_r < Xm_l - D < b_r$. That is, in general the shape of an LDZ is a combination of this type of parallelograms. It is called the "LDZ element" and is plotted in Figure 8, where A, B, C and D are the possible neighboring zero points. The equations $DSMP(A) = 0$, $DSMP(B) = 0$, $DSMP(C) = 0$, and $DSMP(D) = 0$ correspond to the situation $I_L(a_l) = I_r(a_R)$, $I_L(b_l) = I_r(b_R)$, $I_L(a_l) = I_r(b_R)$, and $I_L(b_l) = I_r(a_R)$, respectively. There are four possible cases.

- **Parallelogram:** When $b_l - a_l$ and $b_r - a_r$ are not infinitely small, the corresponding zero region in DSMP is a parallelogram.
- **Line segment perpendicular to Xm_l axis:** When $b_l - a_l$ is 0 but $b_r - a_r$ is not, the parallelogram degenerates to a line perpendicular to the Xm_l axis.
- **Line segment with slope=1:** When $b_l - a_l$ is not infinitely small but $b_r - a_r$ is 0, the parallelogram degenerates to a line with slope=1.

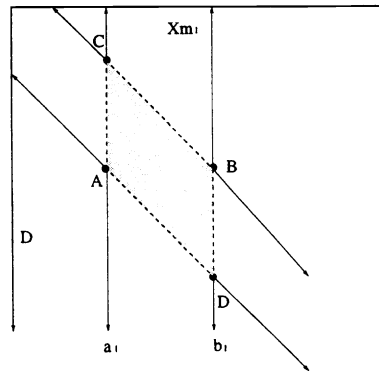


Figure 8. The LDZ element

- **Point:** When both $b_l - a_l$ and $b_r - a_r$ are both zero, the parallelogram degenerates to a point.

Note that two LDZ element connect only through the four vertices, A, B, C and D . An LDZ is a combination of the above four types of LDZ elements. The two cases of "Line segment perpendicular to X_{m_l} axis" and "Line segment with slope=1" hardly occur in the real world.

6.3. Geometric Constraints and Photometric Assumptions on dissimilarity map

When all the above geometric constraints and photometric assumptions are applied to the dissimilarity map, the admissible disparity path can be found by using the following procedure. The matching procedure for disparity path is performed between the conjugate epipolar lines and is restricted by Valid Pairing Constraint.

- **Step 1:** Find the leftmost point in all remaining LDZs.
- **Step 2:** Find the next leftmost point in region VI of the point in Step 1 and repeat this process until the right boundary is reached.
- **Step 3:** *Layer1* path is found. Repeat steps 1 and 2 for the remaining LDZ points until all layers are found.

The above procedure can lead to infinite disparity paths.

6.4. Minimum Occlusion Assumption on the dissimilarity map

The Minimum Occlusion Assumption implies that there is no cross-over occlusion whenever there is a possible matching. In real stereo images, the Minimum Occlusion Assumption also implies the use of non-maximum-LDZ suppression.

The non-maximum-LDZ suppression procedure is to eliminate the LDZs that are contained in another LDZ when viewed from either the left camera or the right camera, as shown in Figure 9(a). Based on this procedure, the repeated texture in a surface can be eliminated. Then possible locations of survived LDZs are illustrated in Figure 9(b). Suppose that z_1 is the LDZ at the left side of the other LDZs, and $z_2, z_3, z_4, z_5, z_6, z_7, z_8$ are the possible LDZs to the right of z_1 .

Next, we try to identify the most likely solutions based on these survived LDZs. We group a set of LDZ's set to represent all the potential disparity paths in this LDZ set. There are many such groups. Then we apply Minimum Occlusion Assumption in these LDZ sets to find the admissible LDZ set (discussed next).

6.5. Depth Smoothness Assumption on the admissible LDZ sets

The Depth Smoothness Assumption assumes that the depth (disparity) should be smooth over the region of smooth intensity. The region with smooth intensity corresponds to an LDZ element of parallelogram shape. The disparity path in the parallelograms which obey the opaque assumption may have infinite solutions. The Depth Smoothness Assumption implies that the disparity path should be a line or a well fit curve across the parallelogram of LDZ.

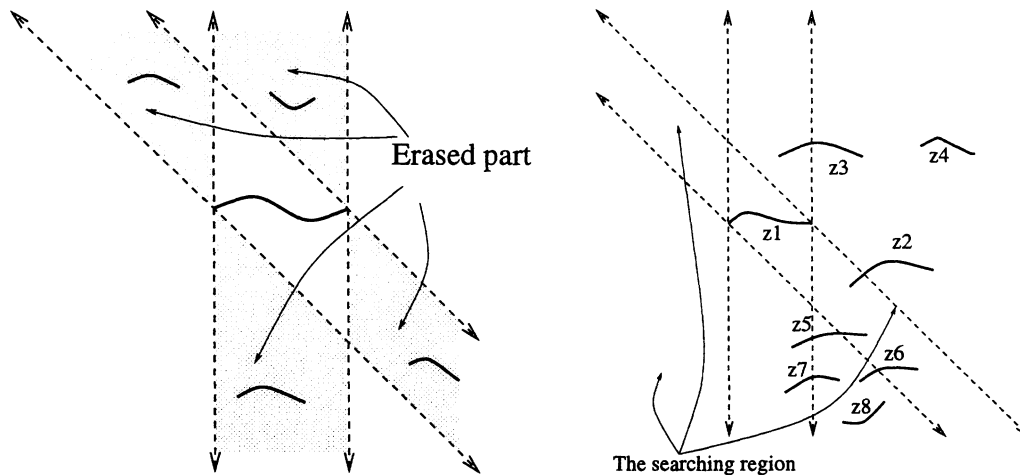


Figure 9. (a) Non-maximum LDZ suppression (b) All combinations of two LDZs

6.6. Statistical criteria on admissible LDZ sets

When there are crossing parts between two neighboring LDZs, there may have infinite possible transition points. The selection of the transition point between two neighboring LDZs may depend on the criteria based on some statistical observations.

7. THE DSMP-BASED METHOD AND SIMULATION RESULTS

7.1. Algorithm

As a first attempt of employing the preceding analysis, we propose the following procedure to find the disparity path on DSMP. The main operation is bounded by the Valid Pairing Constraint and is stated as below.

- **Step 0: DSMP calculation:** We use the mean squared difference for $F(\cdot)$ on a 5×5 window to produce the DSMP.
- **Step 1: LDZ Growing:** A threshold is used to detect the seeds of the LDZs, the areas which has small dissimilarity values. The growing technique is then applied.
- **Step 2: LDZ Merging:** The LDZ may be disconnected due to the noises and non-ideal factors. Hence, the separated LDZs need to be merged together.
- **Step 3: LDZ modeling:** Partition the LDZs into parallelograms and curves.
- **Step 4: Splitting of LDZ:** A detected LDZ may contain more than two LDZs. These merged LDZs should be split.
- **Step 5: Non-maximum-LDZ suppression:** Eliminate the LDZs that are contained in another LDZ when viewed from one of the cameras.
- **Step 6: Formation of the admissible LDZ sets:** Find the multi-layer LDZs.
- **Step 7: Detection of occlusion:** Detect the accurate boundary of occlusion.

In our simulation, Step 5 is executed right after Step1 to reduce computational complexity. The LDZ elements with their disparity range smaller than three are treated as curve. The remaining LDZ elements are treated as parallelograms. When the disparities of the closest two end-points in two neighboring curves within a grown LDZ are different, this LDZ should be split. Occlusions occur between two LDZs. The crossing points between the neighboring

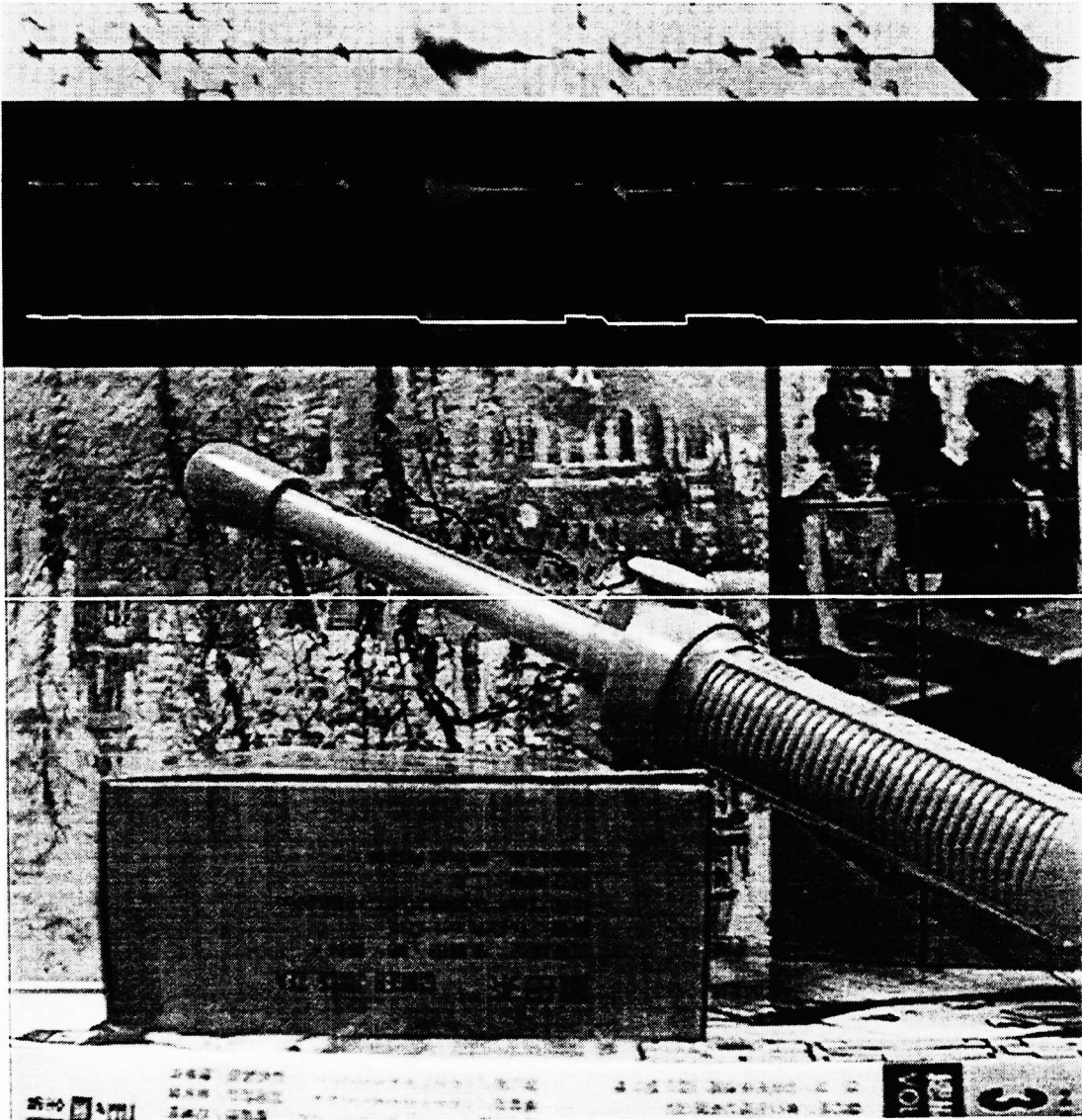


Figure 10. The DSMP, disparity path and original left image

LDZs indicate the location of occlusion. The disparity difference between the neighboring LDZs is the width of the corresponding occlusion. The crossing point is decided by choosing the minimum cost solution along the disparity path between two neighboring LDZs.

7.2. Simulation results

The simulation results are shown in Figure 10, which contains four pictures. The bottom picture is the original left image. The top picture is the DSMP corresponding to the epipolar line shown in the left image. The second picture shows the extraction of LDZs. The third picture shows the decided disparity path. We can find that the disparity path shown in Figure 10 is quite accurate and the occlusions are well detected. In contrast, we show the result using the dynamic programming method⁷ in Figure 11. The disparity path in Figure 11 includes many fake occlusions. The disparity maps generated by these two methods are compared in Figure 12. The DSMP-based method has demonstrated its potential to detect the occlusion more accurately. However, there are still room for improvement. We are currently investigate better implementations of the procedures described at the beginning of this section.

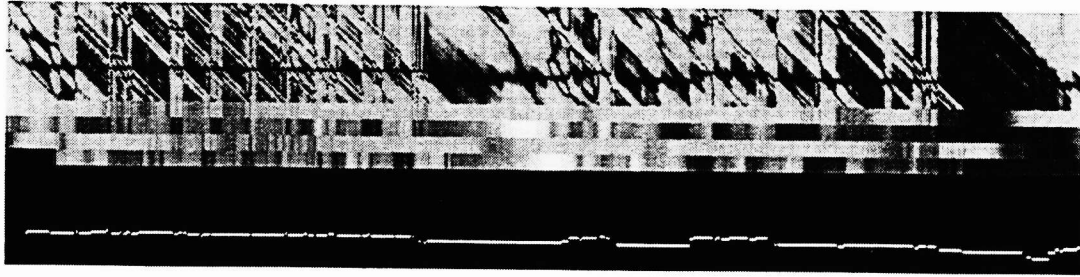
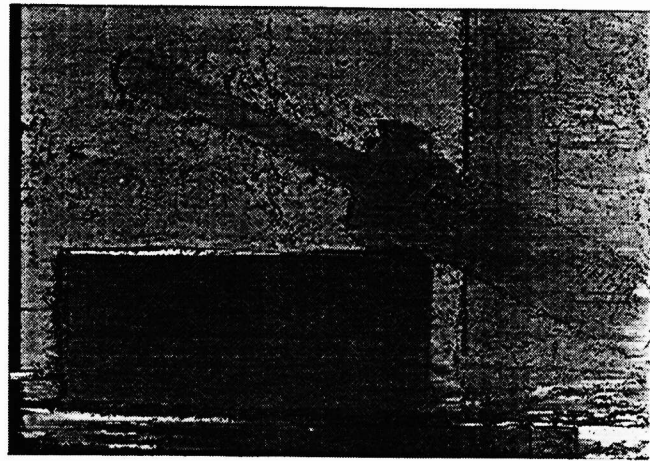


Figure 11. The disparity path of dynamic programming



DSMP-based method



dynamic programming

Figure 12. The disparity maps produced by using DSMP-based method and dynamic programming

REFERENCES

1. E. Krotkov, K. Henriksen and R. Kories, "Stereo Ranging with Verging Cameras," *IEEE Trans. on Pattern Analysis and Machine Intelligence*, pp. 1200-1205, vol. 12, no. 12, December 1990.
2. T. Kanade and M. Okutomi, "A Stereo Matching Algorithm with an Adaptive Window: Theory and Experiment," *Proceedings of the 1991 IEEE International Conference on Robotics and Automation*, pp. 1088-1094, Sacramento, California, April 1991.
3. T. Kanade and M. Okutomi, "A Stereo Matching Algorithm with an Adaptive Window: Theory and Experiment," *IEEE Trans. on Pattern Analysis and Machine Intelligence*, pp. 1628-1634, vol. 16, no. 9, Sep. 1994.
4. Z. N. Le and G. H. Hu, "Analysis of disparity Gradient Based Cooperative Stereo," *IEEE Trans. on Image Processing*, pp. 1493-1506, vol. 5, no. 11, Nov. 1996.
5. T. Y. Chen, A. C. Bovik and L. K. Cormack, "Stereoscopic Ranging by Matching Image Modulations," *IEEE Trans. on Image Processing*, pp 785-797, vol. 8, no. 6, June, 1999.
6. V. S. Nalwa, "A Guided Tour of Computer Vision," *Addison-Wesley Publishing Company*, 1987.
7. I. J. Cox, S. L. Hingorani and S. B. Rao, "A Maximum Likelihood Stereo Algorithm," *Computer Vision and Image Understanding*, Vol. 63, No. 3, pp. 542-567, May, 1996.
8. S. Birchfield and C. Tomasi, "Depth Discontinuities by Pixel-to-Pixel Stereo," *Computer Science Department Stanford Unersiverty*.